

# Tip-shape investigation of a Au–Si alloy liquid metal ion source using a high voltage transmission electron microscope

W Driesel†, Ch Dietzsch† and R Mühle‡

† Max-Planck-Institut für Mikrostrukturphysik, Weinberg 2, D-06120 Halle, Germany

‡ Eidgenössische Technische Hochschule Zürich, Institut für Teilchenphysik, ETH Hönggerberg, CH-8093 Zürich, Switzerland

Received 28 October 1994

**Abstract.** The tip shape of a Au–Si liquid-metal ion source in terms of its dependence on the total ion emission current has been investigated *in situ* in the Halle 1 MeV electron microscope. Within the emission current range 7–90  $\mu\text{A}$  there is a linear dependence of the cone half-angle  $\alpha$  and the length  $l$  of the jet-like protrusion on the increased emission current. The jet-like protrusion at the Taylor cone vertex was not so pronounced as has been observed in the cases of elementary liquid-metal ion sources. No spatial shifts of the Taylor cone are seen during the experiments. In contrast to elementary liquid-metal ion sources, there is no indication of 'Faraday droplets' being emitted from the surroundings of the Taylor cone.

## 1. Introduction

Liquid-metal ion sources (LMISs) have recently found important applications in microelectronics, for example for nanometre-scale device fabrication (Steckl *et al* 1992), the preparation of low-dimensional structures (Hiramoto *et al* 1988), the field of micromachining and device transplantation (Ishitani *et al* 1990) and special analytical techniques such as *in situ* cross sectioning of a specimen for transmission electron microscopy (TEM) from an area selected during scanning ion microscopy (SIM) inspection (Kirk *et al* 1989), or sub-micrometre resolved secondary-ion mass spectroscopy (Levi-Setti *et al* 1985).

For this wide field of application, various kinds of ion species are required. Unfortunately, this type of ion source is applicable only to elements having a relatively low melting point and a low vapour pressure at this point (Broughton and Clampitt 1984, Gamo *et al* 1982). Silicon, which is important for doping GaAs, has a vapour pressure of about  $3 \times 10^{-2}$  Pa at its melting point of 1400 °C. For this reason silicon ions cannot be generated by ionizing elementary silicon in LMISs. The generation of gold ions by an elementary gold LMIS is also not easy because of the high vapour pressure of about  $10^{-3}$  Pa at the melting point of 1063 °C. Therefore a eutectic alloy of Au and Si with 18.6 at% Si, which

melts at only 363 °C, is used to create both Si and Au ions (Gamo *et al* 1981, Komuro 1986, Machalett *et al* 1987). The mass selection between the ion species is usually done by means of a Wien filter.

The possibility of creating both Si and Au ions by means of the same LMIS is also useful in the field of micromachining. Si ions can be used for imaging without notable damage to the specimen and Au ions are very effective for sputtering.

A lot of theoretical work has been done with respect to elementary LMISs, to calculate the shape of the liquid cone (Taylor 1964, Kingham and Swanson 1984a, Forbes and Ljepojevic 1992), to understand better the mechanism of ion emission (Kingham and Swanson 1984b), to calculate the jet length at the Taylor cone vertex (Forbes and Ljepojevic 1992, Mair and Forbes 1992) and to understand the processes of microdroplet emission (Hornsey and Ishitani 1990, Vladimirov *et al* 1993). However, only in a few cases has an operating elementary LMIS been observed *in situ* in a high-voltage transmission electron microscope (HVTEM) (Benassayag *et al* 1985, Denizart *et al* 1991, Hata *et al* 1994). Despite the considerable development of alloy LMISs, the phenomena occurring during source formation and tip-shape evolution with increasing ion current as well as ion and microdroplet emission are still not fully understood. This may be due to the more complex processes involved

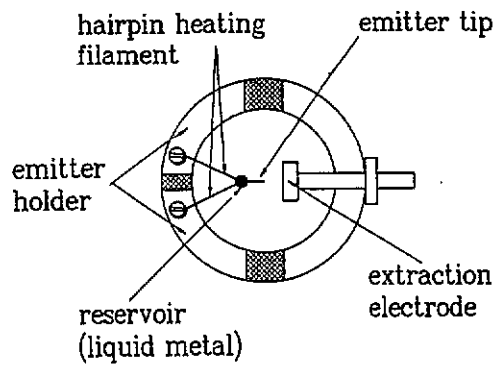


**Figure 1.** The specimen holder used for *in situ* observations of Au–Si alloy liquid-metal ion sources.

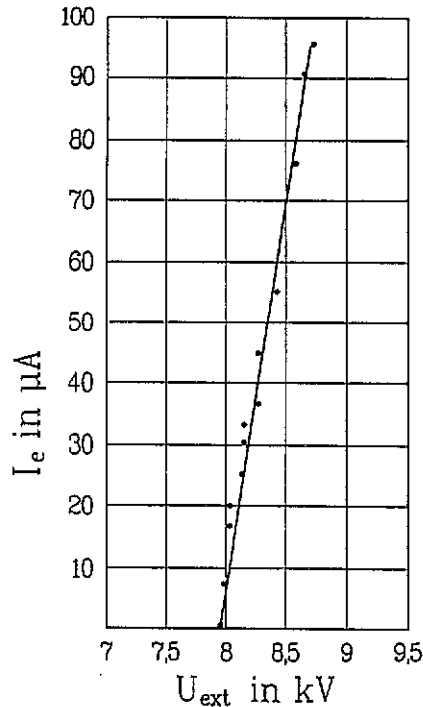


**Figure 2.** Total ion emission current/extraction voltage characteristics.

with alloy LMISs.

For better understanding of the material-dependence of the liquid cone shape and the process of microdroplet emission, we have observed *in situ* in a HVTEM Ga (Driesel *et al* 1994), In (Praprotnik *et al* 1994) and Sn LMISs (Driesel and Dietzsch 1994) all in operation. Also, spatial shifting of the Taylor cone and other instabilities have been investigated in more detail. Most recently some aspects have been studied for the first time concerning the tip shape of a eutectic Au–Si alloy LMIS.

## 2. Experimental

The Au–Si liquid-alloy ion source and the extraction electrode are fitted into the object plane of the 1 MeV HVTEM by means of a special specimen holder (figure 1), which enables one to install the LMIS and the extraction electrode on object level, to connect the LMIS with a high voltage and a heating power supply, and to

bias and measure the current of the extraction electrode during the *in situ* experiments. The distance between emitter tip and extraction electrode is adjustable in the experimental arrangement. A small distance of about 0.5 mm was chosen to reduce the extraction voltage. The Au–Si LMIS used for these experiments consists of a hairpin-like heating filament with a tungsten tip spot-welded to the hairpin. The reservoir of the Au–Si eutectic alloy is formed between the shanks of the hairpin heating filament. The most important part of the emitter, the tungsten tip ( $r \approx 8 \mu\text{m}$ ), was prepared according to the instruction given by Driesel (1993). For the experiments in the HVTEM, only those emitters that had been prepared and tested for their emission capability in another vacuum chamber were used. During the *in situ* experiments in the HVTEM, the environment of the special specimen holder was liquid-nitrogen-cooled to improve the vacuum conditions near the emitter tip ( $p \approx 5 \times 10^{-5} \text{ Pa}$ ), yielding a higher stability of the emission current. The images of the shadow projection of the emitter tip were taken by a photo or video camera.

As the strong electric extraction field between emitter tip and extraction electrode causes deviations of the imaging electron trajectories, a very high acceleration voltage of 1 MV was necessary for the *in situ* experiments in the HVTEM, since the resulting imaging error decreases with increasing acceleration voltage. Our estimations show that this error is approximately 20 nm (Praprotnik *et al* 1994), roughly corresponding to the value given by (Benassayag *et al* 1985) for their experimental arrangement.

## 3. Formation and shape of the Taylor cone

To characterize the emitters used in the *in situ* experiments, the curve in figure 2 shows the total ion emission current measured versus the extraction voltage. To observe changes in the shape of the liquid metal surface on the tungsten tip, the emitter was heated somewhat above the melting point of the Au–Si alloy before the extraction voltage between emitter tip and extraction electrode was increased in small steps from zero up to the onset voltage  $U_c$  of formation of a Taylor cone. Within this voltage range the emitter tip, which is coated with the liquid Au–Si alloy, has a spherical shape, which does not change until the onset voltage of formation of the Taylor cone is reached. The temporal progress of the formation of the Taylor cone is shown in figure 3. As the onset voltage is applied between emitter tip and extraction electrode, the liquid Au–Si alloy is pulled out by the electrostatic forces, which compete with the surface tension forces to form an ellipsoidal shape (figure 3(a)), which immediately changes into the Taylor cone (Taylor 1964), as shown in figure 3(b). The formation steps of the Taylor cone cannot be resolved temporally, because the formation process of the cone is much faster than the picture frequency (TV norm) used during video recording. It was possible to measure the height of the Taylor cone from figures 3(b)–(d). For that

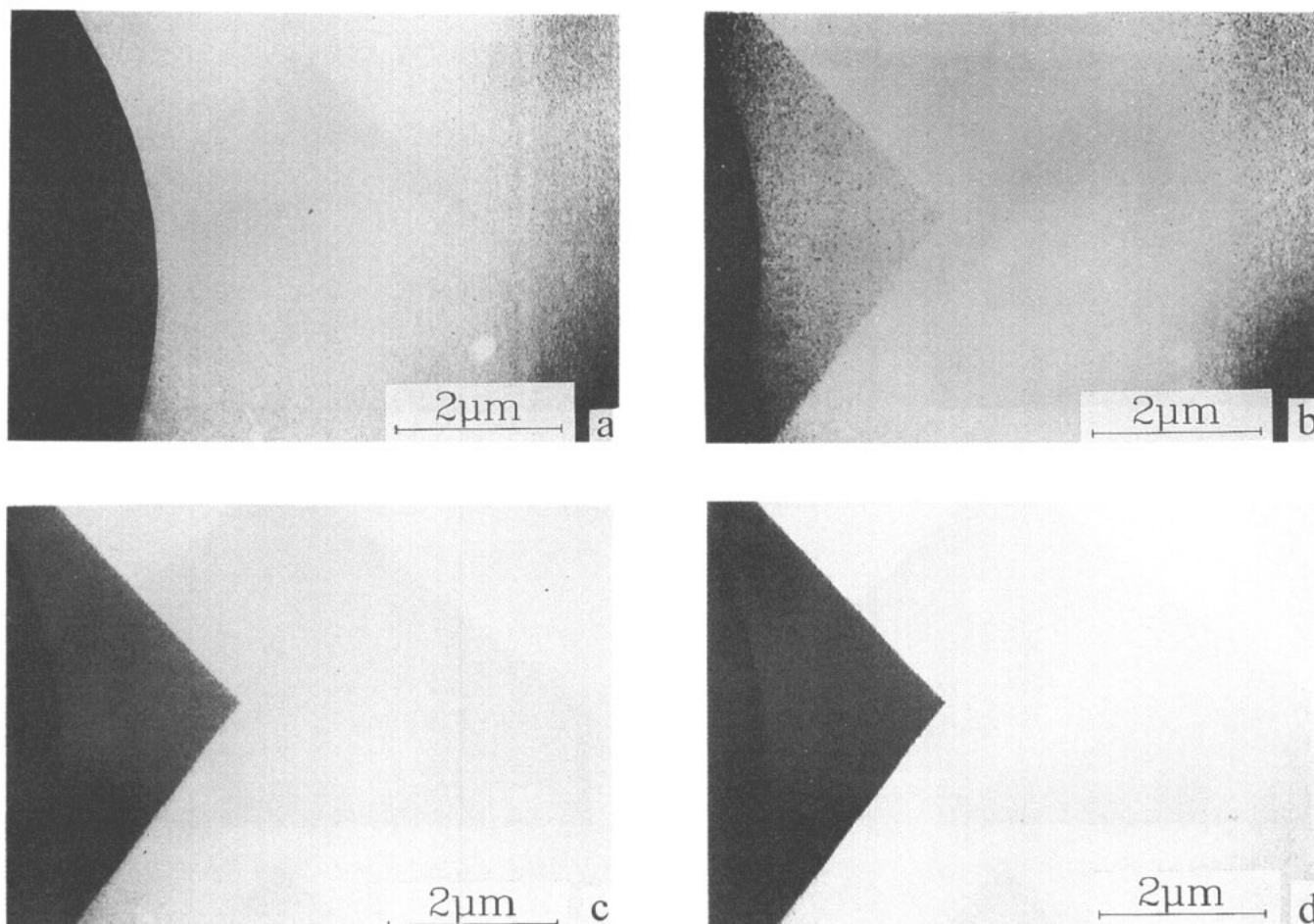


**Figure 3.** The formation of the Taylor cone. The images were copied from the video film and temporally sorted: (a) the image without the Taylor cone, (b) the liquid surface after 0.02 s (the Taylor cone has already formed), (c) the liquid surface shape after 0.06 s and (d) the liquid surfaces shape under stable ion emission conditions after 0.14 s.

**Table 1.** The dependence of the cone half-angle  $\alpha$  and length  $l$  of the jet-like protrusion on the emission current  $I_e$  with  $\Delta I_e = \pm 0.5 \mu\text{A}$ ,  $\Delta\alpha = \pm 0.5^\circ$  and  $\Delta l = \pm 20 \text{ nm}$ .

$I_e$ ( $\mu\text{A}$ )	$\alpha$ (degrees)	$l$ (nm)
7	49.3	20
16	48.5	30
20	48.0	50
25	48.0	75
30	47.0	90
33	46.0	110
36	45.5	120
45	45.0	120
55	45.0	150
76	45.0	200
90	43.0	300
95	42.0	450

purpose the afterglow of the CCD camera, which caused superimposed contours of the spherical surface shape and of the cone, was used. The height of the Taylor cone at the onset voltage amounts to  $2.17 \mu\text{m}$ . Varying the extraction voltage caused a shift of the image. Therefore it was not possible to determine the dependence of the

cone height on the ion emission current.

Figures 4 and 5 show the shape of the Taylor cone's dependence on the ion emission current. Table 1 lists all the values measured of both cone half-angle  $\alpha$  and jet length  $l$  in terms of their dependence on the ion emission current  $I_e$ .

The cone half-angle  $\alpha$  of the liquid cone decreases from  $\alpha = 49.3^\circ$  to  $42.0^\circ$  with increasing emission current  $I_e$ . The length  $l$  of the jet-like protrusion, which is measured from the apex of the underlying Taylor cone (figure 6), increases with increasing ion emission current  $I_e$ . The experiments show that an increase in extraction voltage is not only compensated by an increase in jet length, but also by a decrease in the cone half-angle  $\alpha$ .

At higher emission currents ( $I_e \geq 90 \mu\text{A}$ ) the cone walls of the Taylor cone become increasingly concave (figure 5(f)) so that a linear approximation defining the cone half-angle  $\alpha$  becomes less correct. Therefore only the ion current range between onset current and  $90 \mu\text{A}$  (table 1) is used to reveal the correlation between cone half-angle  $\alpha$ , jet length  $l$  and current  $I_e$ , respectively. The graph of figure 7(a) shows the asymptotic cone half-angle  $\alpha$ , whereas that of figure 7(b) illustrates the dependence of the measured length  $l$  of the jet-like

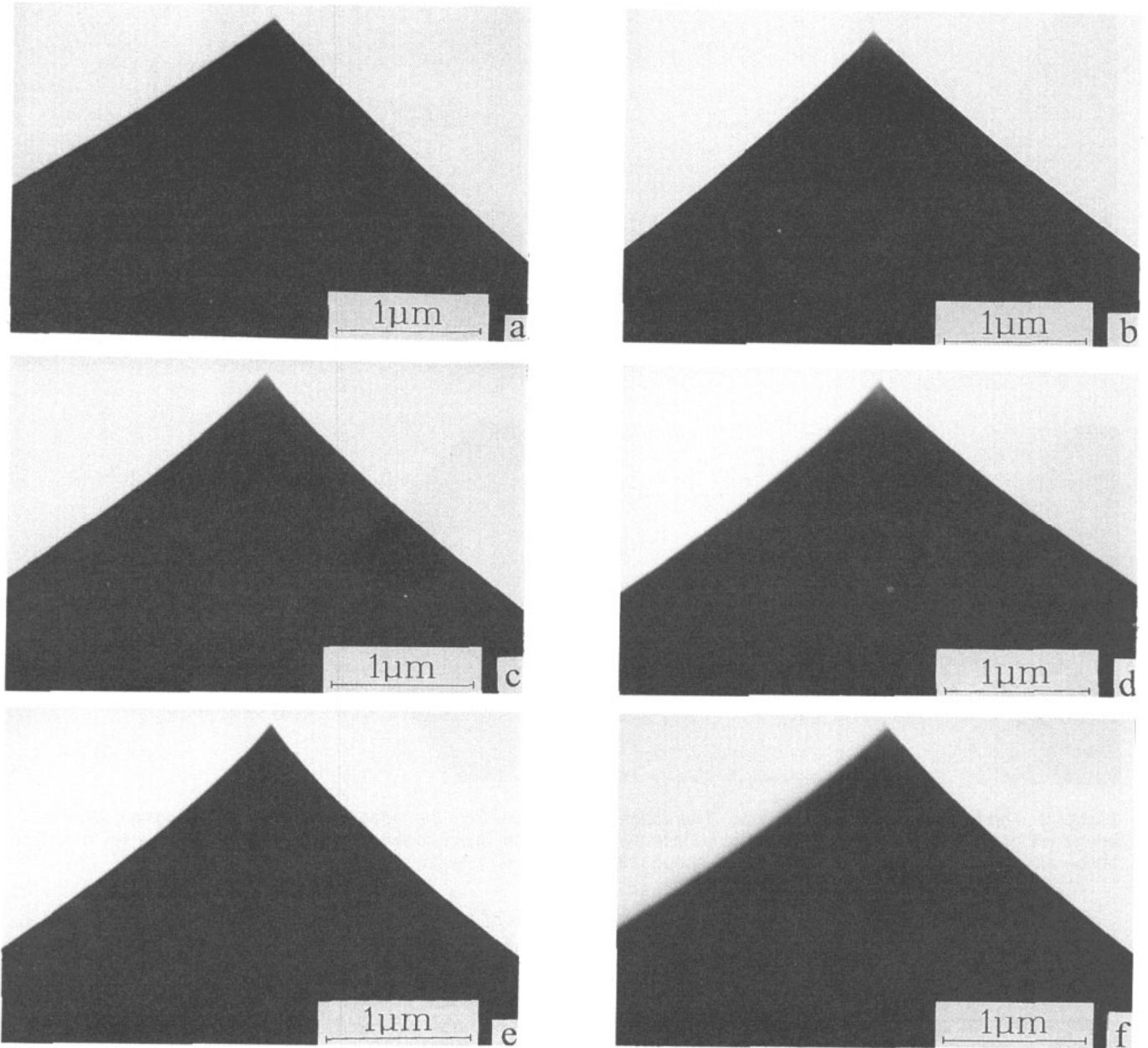


**Figure 4.** The shape of the Taylor cone for different ion emission currents: (a)  $I_e = 7 \mu\text{A}$ , (b)  $I_e = 16 \mu\text{A}$ , (c)  $I_e = 20 \mu\text{A}$ , (d)  $I_e = 25 \mu\text{A}$ , (e)  $I_e = 30 \mu\text{A}$  and (f)  $I_e = 33 \mu\text{A}$ .

**Table 2.** The linear dependencies of cone half-angle  $\alpha$  and length  $l$  of the jet-like protrusion measured for Au–Si, Ga, In and Sn liquid-metal ion sources.

	$\alpha_0$ (degrees)	$d\alpha/dI_e$ (degrees $\mu\text{A}^{-1}$ )	$l_0$ (nm)	$dl/dI_e$ (nm $\mu\text{A}^{-1}$ )
Au–Si	49.1	0.07	$\approx 0$	3
Ga	53.5	0.129	$\approx 0$	4.4
In	51.1	0.298	-230	39
Sn	50.5	0.15	$\approx 0$	12

protrusion on the emission current  $I_e$ . The fitted curves are calculated by using the following expressions:

$$\alpha = \alpha_0 - (d\alpha/dI_e)I_e \quad \alpha_0 = 49.1^\circ$$

$$d\alpha/dI_e = 0.07 \mu\text{A}^{-1}$$

$$l = l_0 + (dl/dI_e)I_e \quad l_0 = 0 \text{ nm}$$

$$dl/dI_e = 3 \text{ nm } \mu\text{A}^{-1}.$$

Similar dependencies (table 2) were revealed by *in situ* HVTEM investigations of Ga (Driesel et al 1994), In (Praprotnik et al 1994) and Sn LMISs (Driesel and Dietzsch 1994). These experimental results show that the change of both cone half-angle  $\alpha$  and jet length  $l$  is most pronounced for the In LMIS. The appearance of a plateau for the cone half-angle  $\alpha$  for medium currents in figure 7(a) and the sharp increase in the jet length  $l$  for high emission currents in figure 7(b) require further investigation.

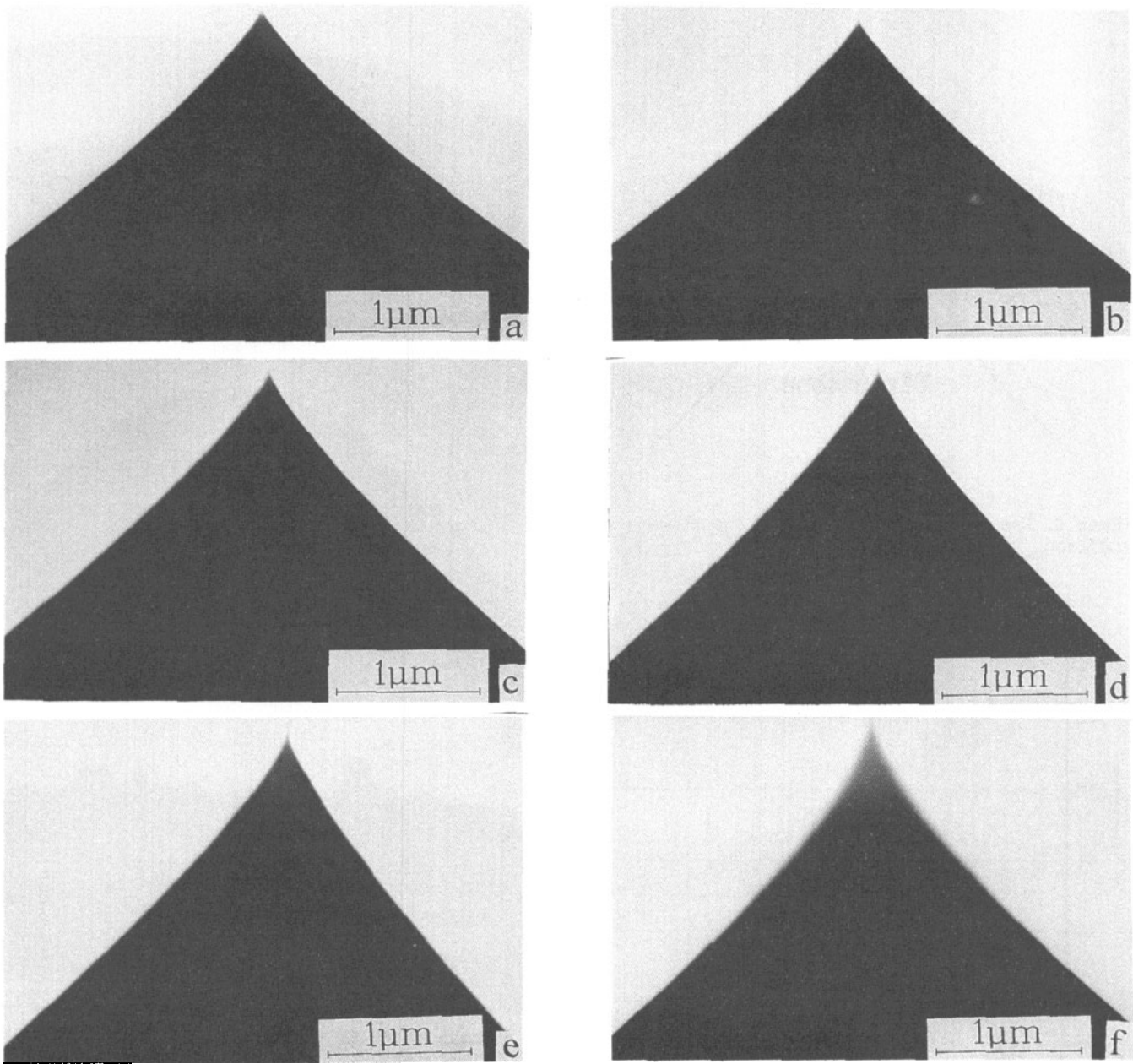


**Figure 5.** The shape of the Taylor cone for different ion emission currents: (a)  $I_e = 36 \mu\text{A}$ , (b)  $I_e = 45 \mu\text{A}$ , (c)  $I_e = 55 \mu\text{A}$ , (d)  $I_e = 76 \mu\text{A}$ , (e)  $I_e = 90 \mu\text{A}$  and (f)  $I_e = 95 \mu\text{A}$ .

The differences in both cone half-angle and jet length measured between the Au–Si alloy LMIS and the elementary LMISs give further experimental evidence of a material-dependence of the Taylor cone shape. The cone half-angle  $\alpha$  decreases by a factor of 0.235 relative to that of an In emitter, and the length  $l$  of the jet-like protrusion increases by less than one order of magnitude compared with the change for the case of the In emitter. One reason for this material-dependence may be the different space-charge-induced depression of the surface field. A second reason could be the difference in the surface tension between the different elements or alloys, which may influence the cone shape and the jet length (Mair and Forbes 1992) too.

#### 4. Instabilities and emission of microdroplets

During the *in situ* experiments, we investigated oscillations of the Taylor cone at the onset voltage. Video recordings illustrate these processes.

It is well known from earlier investigations on elementary LMISs (Driesel *et al* 1994, Driesel and Dietzsch 1994, Praprotnik *et al* 1994) that there was a strong emission of large microdroplets from the surroundings of the Taylor cone. The Au–Si alloy LMIS shows another behaviour. At the beginning of the experiments, the liquid surface in the vicinity of the Taylor cone is smooth (figure 8(a)). There is no indication of large droplets being emitted at the emission areas of ‘Faraday droplets’ as was observed

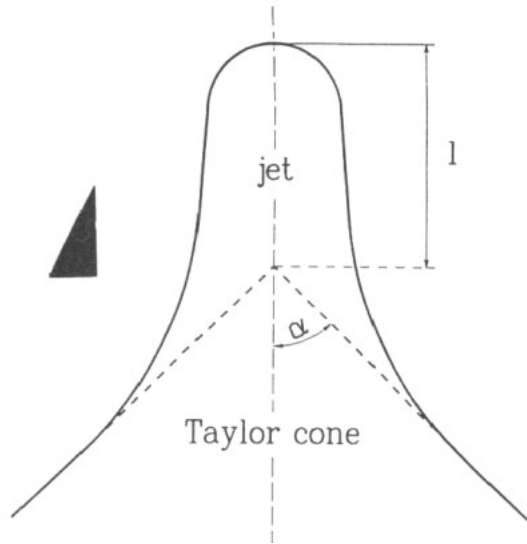


**Figure 6.** The scheme of the Taylor cone and jet-like protrusion.

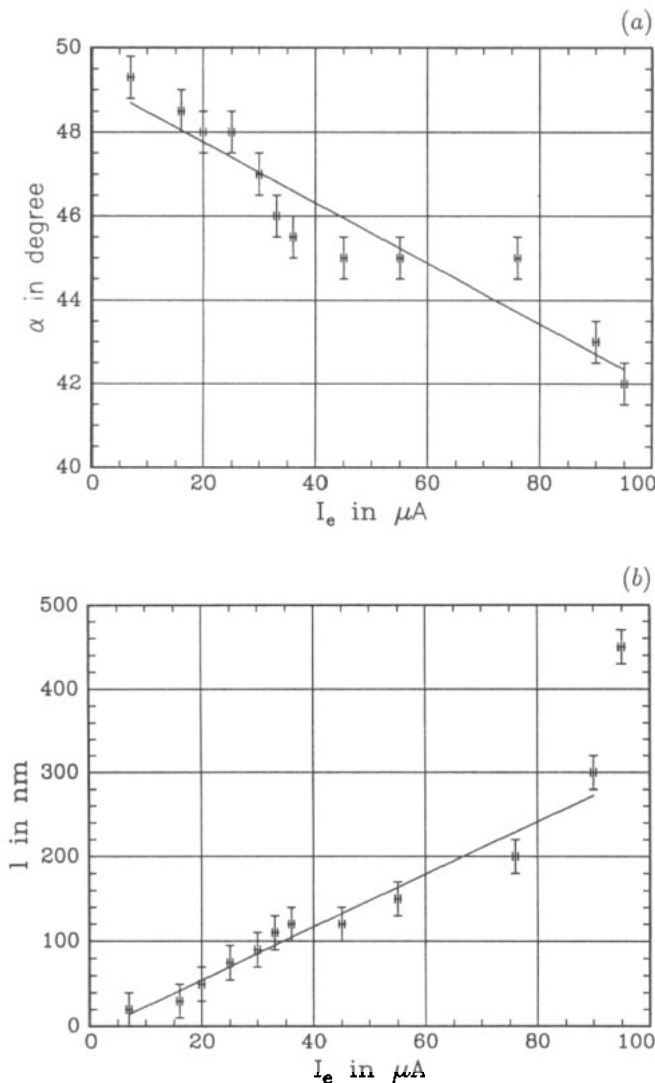


**Figure 7.** (a) The dependence of the cone half-angle  $\alpha$  on ion emission current  $I_e$ . (b) The dependence of the jet length  $l$  on ion emission current  $I_e$ .

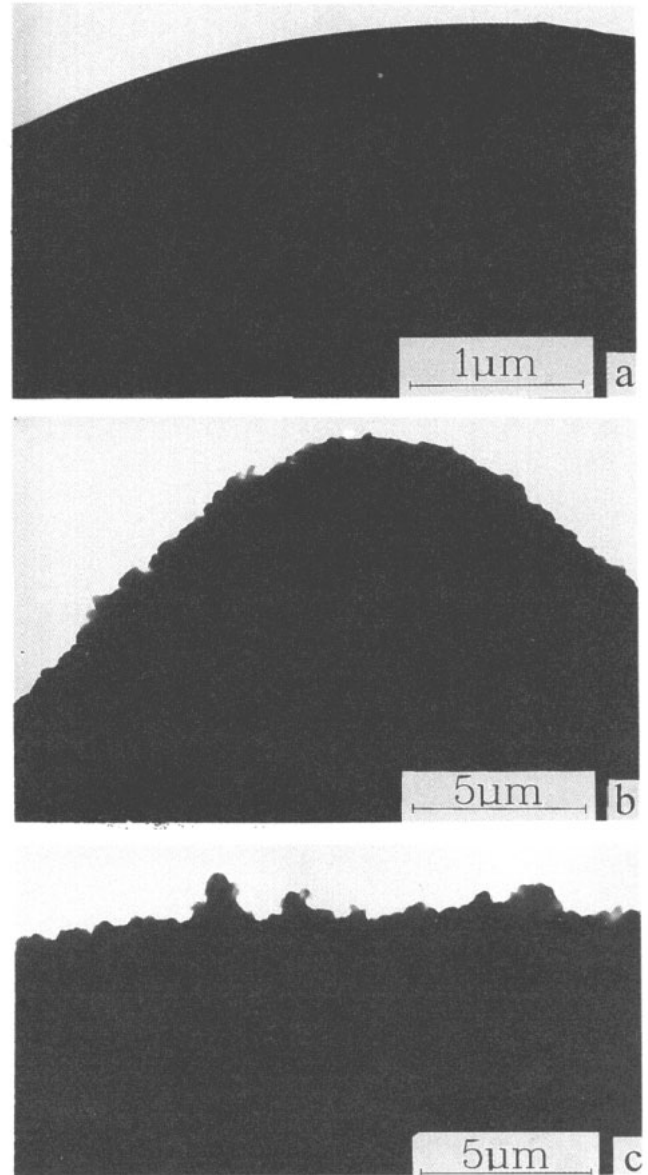


**Figure 8.** The change in the surface roughness during ion emission: (a) after a short working time of only a few minutes, (b) and (c) after operating for about 8 h.

for elementary LMISs during the experiments. After an operating time of about 8 h in the HVTEM there was a change in the topography for the surface (figures 8(b) and (c)), which may be due to a change in the surface composition or to poisoning of the LMIS. This result may be an indication of an alteration in the properties of the Au-Si alloy LMIS. Further experiments will be necessary in order to clarify this issue.

### 5. Electron emission from a Au-Si liquid-metal ion source

As the process of Taylor cone formation is independent of the polarity of the extraction voltage, one might speculate about whether or not it is possible to achieve stable DC field electron emission by applying reversed polarity to the LMIS as has been reported by other



authors (Swanson and Schwind 1978, Hata *et al* 1987). Therefore the tip shape of an Au–Si liquid-metal emitter has been observed *in situ* also in the case of reversed polarity in terms of its dependence on the extraction voltage. Increasing the extraction voltage between emitter and extraction electrode in small steps up to the onset voltage of the formation of the Taylor cone for a short time causes an ellipsoidal tip shape, followed by pulse-like electron emission. No formation of a stable Taylor cone has been revealed.

## 6. Conclusions

The formation of the Au–Si liquid alloy cone has been observed *in situ* in the Halle HVTEM. The cone half-angle decreases linearly with increasing emission current. At an emission current of  $I_e \approx 7 \mu\text{A}$  there is an additional jet-like protrusion at the Taylor cone vertex, which increases in length with increasing emission current. The cone half-angle  $\alpha$  of the liquid cone decreases from  $\alpha = 49.3^\circ$  to  $42.0^\circ$  with increasing emission current  $I_e$ . At emission currents higher than  $90 \mu\text{A}$ , the shape of the liquid cone further changes, making the estimation of the asymptotic cone half-angle difficult. The emission of 'Faraday droplets' has not been observed in the surroundings of the Taylor cone. On applying Au–Si liquid-metal emitters in the electron emission mode, in no case was the formation of a stable liquid cone observed.

## Acknowledgments

The authors would like to thank Professor J Heydenreich of the Max-Planck-Institut für Mikrostrukturphysik Halle and Dr R G Forbes of the University of Surrey for stimulating discussions. Moreover, thanks are due to Dr F Machalet of the Friedrich-Schiller-Universität Jena for providing the Au–Si alloys and Mrs F Pabisch of the Max-Planck-Institut für Mikrostrukturphysik Halle for her careful technical

assistance during the experiments and for preparing and testing the LMISs. Dr Driesel would like to thank the Deutsche Forschungsgemeinschaft for their support of these investigations.

## References

- Benassayag G, Sudraud P and Jouffrey B 1985 *Ultramicroscopy* **16** 1
- Broughton and Clampitt 1984 *Vacuum* **34** 275
- Denizart M, Hadeff B, Soum G and Verdier P 1991 *Optik* **88** 7
- Driesel W 1993 *Ultramicroscopy* **52** 65
- Driesel W and Dietzsch Ch 1994 to be published
- Driesel W, Dietzsch Ch, Niedrig H and Praprotnik B 1994 *Ultramicroscopy* submitted
- Forbes R G and Ljepejevic N N 1992 *Surf. Sci.* **266** 170
- Gamo K, Inomoto Y, Ochiai Y and Namba S 1982 *Proc. 10th Int. Conf. Electron and Ion Beam Science and Technology* ed R Bakish (Montréal: Electrochemical Society) p 461
- Gamo K, Ukegawa T, Inomoto Y, Ochiai Y and Namba S 1981 *J. Vac. Sci. Technol.* **19** 1182
- Hata K, Ohya R, Nishigaki S, Tamura H and Noda T 1987 *Japan. J. Appl. Phys.* **26** L896
- Hata K, Saitoh Y, Oshita A, Takeda M, Morita C and Noda T 1994 *Appl. Surf. Sci.* **76/77** 36
- Hiramoto T, Hirakawa K and Ikoma T 1988 *J. Vac. Sci. Technol.* **6** 1014
- Hornsey R and Ishitani T 1990 *Japan. J. Appl. Phys.* **29** L1007
- Ishitani T, Ohnishi T and Kawanami Y 1990 *Japan. J. Appl. Phys.* **29** 2283
- Kingham D R and Swanson L W 1984a *J. Physique C* **9** 133
- 1984b *Appl. Phys. A* **34** 123
- Kirk E C G, Williams D A and Ahmed H 1989 *Inst. Phys. Conf. Ser.* **100** 501
- Komuro M 1986 *Japan. J. Appl. Phys.* **25** 1500
- Levi-Setti R, Crow G and Wang Y L 1985 *SEM 1985* vol II, p 535
- Machalett F, Mühle R and Stiebritz I 1987 *J. Phys. D: Appl. Phys.* **20** 1417
- Mair G L R and Forbes R G 1992 *Surf. Sci.* **266** 180
- Praprotnik B, Driesel W, Dietzsch Ch and Niedrig H 1994 *Surf. Sci.* **314** 353
- Steckl A J, Mogul H C and Mogren S 1992 *Appl. Phys. Lett.* **60** 1833
- Swanson L W and Schwind G A 1978 *J. Appl. Phys.* **49** 5655
- Taylor G I 1964 *Proc. R. Soc. A* **280** 383
- Vladimirov V V, Badan V E, Gorshkov V N and Soloshenko I A 1993 *Appl. Surf. Sci.* **65/66** 1